Round-trip imaging through scattering media based on optical transmission matrix

Bin Zhuang (庄 斌)[1,2], **Chengfang Xu (许程访)**[1,2,3], **Yi Geng (耿 燚)**[1,2],
Guangzhi Zhao (赵广智)[1,2], **Hui Chen (陈 慧)**[1,2], **Zhengquan He (贺正权)**[1],
Zhaoxin Wu (吴朝新)[3], **and Liyong Ren (任立勇)**[1,*]

[1]*Research Department of Information Photonics, Xi'an Institute of Optics and Precision Mechanics,*
Chinese Academy of Sciences, Xi'an 710119, China
[2]*University of Chinese Academy of Sciences, Beijing 100049, China*
[3]*Department of Electronics Science and Technology, School of Electronic & Information Engineering,*
Xi'an Jiaotong University, Xi'an 710049, China
*Corresponding author: renliy@opt.ac.cn

Traditional one-way imaging methods become invalid when a target object is completely hidden behind scattering media. In this case, it has been much more challenging, since the light wave is distorted twice. To solve this problem, we propose an imaging method, so-called round-trip imaging, based on the optical transmission matrix of the scattering medium. We show that the object can be recovered directly from the distorted output wave, where no scanning is required during the imaging process. We predict that this method might improve the imaging speed and have potential application for real-time imaging.

OCIS codes: 110.0113, 110.1650, 110.1758, 110.6150.
doi: 10.3788/COL201816.041102.

The inhomogeneity of scattering media distorts the propagation of light waves, which diverts the propagation direction and disorders the spatial relationship of rays from the object. As a consequence, the optical image may be highly deteriorated or disappear entirely. In recent years, a number of methods[1–19], for instance, computational ghost imaging, wavefront shaping, speckle correlation, and optical transmission matrix (TM), have been proposed to solve this seemingly intractable problem caused by turbidity. They are verified to be effective in the one-way imaging case, i.e., the transmission imaging. Nevertheless, it will become more challenging to image an object that is completely hidden behind the scattering medium, because an active light source is needed to illuminate the object through the scattering medium. In such a case, the light wave will be distorted twice: on the way in for the illumination and on the way out for the detection. Therefore, we hereby call it the round-trip imaging in this Letter. Note that such an imaging operation is actually working in the reflection imaging mode instead of the one-way imaging working in the transmission imaging mode.

Indeed, the computational ghost imaging method is widely used to image an object through the scattering medium[1–4], but it is not effective to the round-trip imaging, since the illumination wave is strongly distorted after passing through the scattering medium. Although the wavefront shaping has been demonstrated as a powerful technique for focusing and imaging through the scattering medium[5–8], its scanning process is very time-consuming, making it not suitable for real-time imaging. Meanwhile, the speckle correlation method has gotten development recently, owing to its ability of single-shot imaging[9–11], but it

relies on the "memory-effect" for the speckle correlation, which limits its application to the cases of thin scattering media and small viewing angles. Moreover, the optical TM inherently characterizes the scattering medium by giving the relationship between the input wave and the output wave in advance[12], and then it can be used to directly recover the object wave for imaging from the distorted detected wave. Recently, based on its excellent performance in focusing and imaging, this method has gotten developed from the monotonous effects[13–16] to the multispectral[17] or polychromatic effects[18] and the polarization effects[19]. Furthermore, the nonlinear[20] and acoustic effects[21] have also been studied and expected to achieve reflective imaging. Nevertheless, generally speaking, so far these studies are still only developed to overcome the one-way distortion for transmission imaging, and it is not effective for the round-trip imaging, where the illumination wave has already been highly deteriorated due to the on-the-way-in distortion. In order to overcome such a distortion, some extra technologies are usually adopted, which inevitably make the experiment procedure complicated and unstable. For example, the speckle imaging technology has ever been widely adopted for this purpose, but this technology involves an average process of a large number of speckle images[22,23].

In this Letter, in order to overcome the on-the-way-out distortion and eliminate the influence of the on-the-way-in distortion simultaneously, we propose and establish the round-trip imaging scheme based on measuring the round-trip TM of the scattering medium. The experiment procedure to acquire the round-trip TM is introduced, and the object recovering results from the distorted output wave with this TM are also demonstrated.
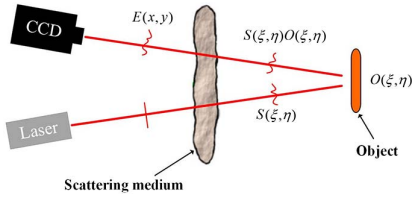
Fig. 1. Schematic of the round-trip imaging through a scattering medium.

As shown in Fig. 1, when imaging an object that is hidden behind a scattering medium, a round-trip imaging is performed, in which the incident plane wave has been distorted twice by the scattering medium.

Theoretically, the final output wave detected by CCD can be expressed as

$$E(x, y) = \sum_{\xi, \eta} K(x, y; \xi, \eta) S(\xi, \eta) O(\xi, \eta), \quad (1)$$

where $O(\xi, \eta)$ is the complex amplitude of the target object, and $S(\xi, \eta)$ is the illumination wave whose light field distribution becomes unknown due to the on-the-way-in distortion via the scattering medium. Based on these definitions, the light waves reflected by the object can be described as $S(\xi, \eta) O(\xi, \eta)$.

Note that, in Eq. (1), $K(x, y; \xi, \eta)$ is the traditional one-way TM of the scattering medium, which gives the relationship between the reflected wave $S(\xi, \eta) O(\xi, \eta)$ and the output wave $E(x, y)$. As long as $K(x, y; \xi, \eta)$ is measured, $S(\xi, \eta) O(\xi, \eta)$ can be recovered from $E(x, y)$. However, we cannot recover the object $O(\xi, \eta)$ yet, since $S(\xi, \eta)$ is still unknown. To solve this problem, specially, we define

$$T(x, y; \xi, \eta) = K(x, y; \xi, \eta) S(\xi, \eta), \quad (2)$$

as the round-trip TM of the scattering medium. It is seen from Eq. (2) that, different from the one-way TM $K(x, y; \xi, \eta)$, this TM $T(x, y; \xi, \eta)$ has additionally recorded the distorted field distribution of the illumination wave $S(\xi, \eta)$. In this way, Eq. (1) becomes

$$E(x, y) = \sum_{\xi, \eta} T(x, y; \xi, \eta) O(\xi, \eta). \quad (3)$$

Note that once $T(x, y; \xi, \eta)$ is measured, the relationship between the object and the output wave is given. As a result, the object information $O(\xi, \eta)$ can be recovered directly from the output wave $E(x, y)$ through the following phase conjugation operation[14]:

$$O_{\mathrm{rec}}(\xi, \eta) = \frac{\langle T^*(x, y; \xi, \eta) E(x, y) \rangle_{x,y}}{\langle T^*(x, y; \xi, \eta) T(x, y; \xi, \eta) \rangle_{x,y}}, \quad (4)$$

where T^* is the complex conjugation of the TM element, and $\langle \cdot \rangle_{x,y}$ means the spatial average over the entire image plane.
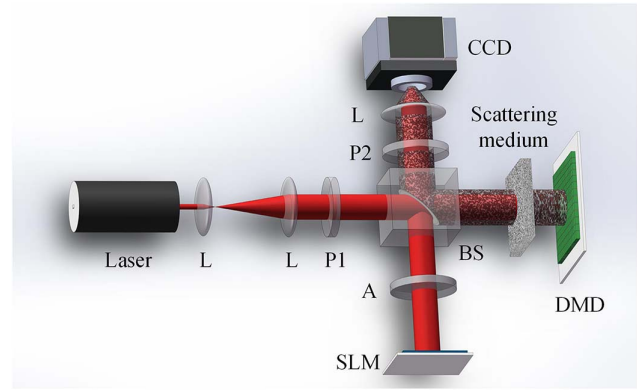

Fig. 2. Experimental setup. Scattering medium (Thorlabs Optics 220 grit ground-glass diffuser); DMD, digital micromirror devices (ViALUX, V-7001VIS, 1024 pixel × 768 pixel); SLM, spatial light modulator (Meadowlark Optics, P1920-0635-HDMI); CCD (Hamamatsu, C13440-20CU, 2048 pixel × 2048 pixel, the central 2048 pixel × 1536 pixel area is used for imaging); L, lens; P, polarizer; BS, beam splitter; A, attenuation film.

The experimental setup is shown in Fig. 2. A He–Ne laser with a wavelength of 632.8 nm is expanded and split into two beams by a beam splitter (BS). The reflected beam is modulated and reflected by the spatial light modulator (SLM) to produce the reference wave, while the transmitted beam, via the distortion by the scattering medium, illuminates the digital micromirror device (DMD) on the way in; then, the reflected wave by DMD is distorted again by the scattering medium on the way out to produce the output wave. Finally, the interference image of these two waves is recorded by a CCD.

To measure $T(x, y; \xi, \eta)$, we divide the DMD into 64×48 segments (the size of each segment: 219 μm × 219 μm) and select the central 32×24 segments for imaging. We turn on only one segment of the DMD in sequence and change the phase of the reference wave by the SLM; the output wave is measured by using the phase-shifting digital holography technology[24]. The typical elements of $T(x, y; \xi, \eta)$ are shown in Figs. 3(a) and 3(b) for the amplitude part and the phase part, respectively. Obviously, both the amplitude and the phase are strongly speckled. It should be pointed out that the measured $T(x, y; \xi, \eta)$ actually has the ability to eliminate the influence of the on-the-way-in distortion; this is
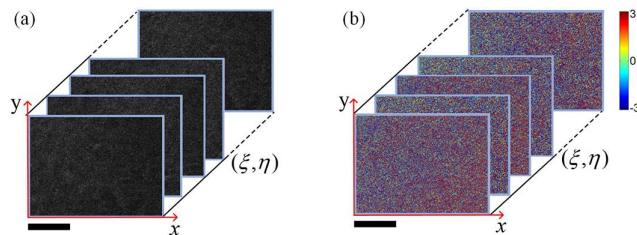

Fig. 3. Typical measured $T(x, y; \xi, \eta)$ elements. (a) Amplitude and (b) corresponding phase, respectively. Scale bars: 4000 μm; color bar: phase in radian.

owing to the fact that the light field of the illumination wave has already been recorded in the round-trip TM.

After completely measuring the $T(x, y; \xi, \eta)$, in what follows, we will show the imaging results through the following two experiments.

Firstly, taking into account the stability of the system, the target object is also constructed by the DMD. The binary amplitude target object is shown as Fig. 4(a), where the reflectivity of the background and that of the characters are 0.8 and 1.0, respectively. Figure 4(b) is the output speckle image of the object captured by the CCD (the wave at the reference arm is blocked here). It is seen from Fig. 4(b) that the object wave has been seriously distorted by the scattering medium, so it is impossible to image the object directly. Figure 4(c) is the interference image of the object wave and the reference wave. Figures 4(d) and 4(e) are the amplitude and the phase of $E(x, y)$ measured by using the phase-shifting digital holography technology. With $T(x, y; \xi, \eta)$ being measured previously, the recovered object, shown in Fig. 4(f), is obtained from $E(x, y)$ by Eq. (4).

Secondly, in order to show that our method has the ability to image the real object, the DMD is removed, and the USAF 1951 resolution chart is used as the test target. As shown in Fig. 5(a), the pattern whose resolution is 2.24-line-pair/mm is chosen as the imaging area (unit size 223 μm, close to the TM unit of 219 μm). Similarly, the output image of the object shown in Fig. 5(b) is seriously speckled, and the reconstructed result is shown in Fig. 5(c). It is seen that the imaging quality is not as good as the result obtained in the first experiment. We owe this deficiency to two reasons: firstly, the movement of the DMD and the resolution chart has influenced the stability of the system; secondly, the inconsistent unit size between the TM (219 μm) and the resolution chart (223 μm) will also aggravate the imaging error.

To further verify the validation of our round-trip TM method, firstly, we record the speckle pattern of the illumination wave by placing a CCD at the position of the DMD; the result is shown in Fig. 6(a). It is seen that

Fig. 5. Reconstruction of the real target object. (a) USAF 1951 test pattern. (b) Output speckle image of the object. (c) Recovered object. Scale bars indicate 300 μm in (a), (c), and 2000 μm in (b).

Fig. 6. (a) Speckle pattern of the illumination wave. (b) Object constructed using the DMD. (c) Intensity of the reflected wave of the object. Scale bar: 1000 μm.

the originally uniformed incident light is seriously distorted due to the on-the-way-in process via the scattering medium. Note that this wavefront distortion aggravates the difficulty to the subsequent imaging retrieval. Furthermore, we multiply the object [shown in Fig. 6(b)] by the speckle pattern [shown in Fig. 6(a)] to indicate the intensity of the reflected wave of the object indirectly (corresponding to $S(\xi, \eta)O(\xi, \eta)$ in Fig. 1). The result is shown in Fig. 6(c). It is seen that the information of the object $O(\xi, \eta)$ is completely submerged. This means that, even adopting the traditional one-way imaging method using the one-way TM, only Fig. 6(c) might be the best recovery result instead of the Fig. 4(f), which could be obtained by adopting our round-trip imaging method using the round-trip TM.

In conclusion, in order to image an object that is completely hidden behind a scattering medium, we propose a round-trip imaging method based on the round-trip TM. Different from the traditional one-way TM, such a round-trip TM is not only useful to overcome the on-the-way-out distortion but also has the ability to eliminate the influence of the on-the-way-in distortion. In this way, the object can be recovered directly from the distorted output wave. Compared with other methods[5–11], our method has the ability to image the rapid movement objects, since no scanning is involved during the imaging process. What is more, it also works well for thick scattering media, since it does not rely on the inherent characteristics of the medium, for instance the "memory-effect" used in the speckle correlation method. In this Letter, for simplicity, we only imaged a pure amplitude object, but since we have gotten the complex amplitude (amplitude and phase) of the TM and the distorted output wave, our method can also recover the phase of the object simultaneously. That is to say, it can be applied to imaging the complex amplitude object.

Nowadays, our method still faces a huge challenge, as the DMD must be embedded behind the scattering medium in advance to acquire the round-trip TM.
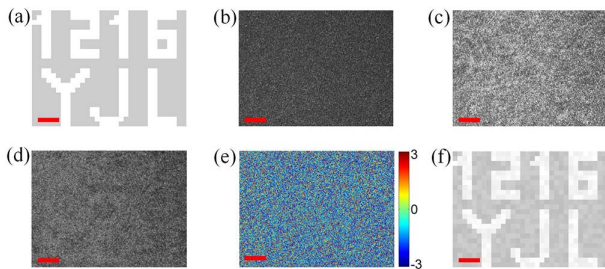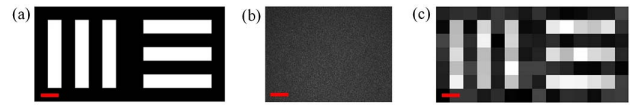
Fig. 4. Reconstruction of the object constructed by DMD. (a) A binary amplitude object constructed by using DMD. (b) Output speckle image of the object captured by CCD. (c) Interference image of the object wave and the reference wave. (d), (e) Amplitude and phase of $E(x, y)$, respectively. (f) Recovered object. Scale bars indicate 1000 μm in (a), (f) and 2000 μm in (b), (c), (d), (e). Color bar: phase in radian.

This prevents us from achieving the non-invasive imaging, e.g., biomedical imaging. Nevertheless, our method still has potential applications in some other cases. On one hand, one can monitor the target through an apparently opaque screen (used as a barrier), while it is incapable of being observed by it. On the other hand, one can also use the scattering medium as an imaging sensor instead of a barrier for imaging. For example, the single multimode optical fiber as a scattering medium shows potential applications for endoscopic imaging, owing to its smaller diameter[23,25–27].

References

1. J. H. Shapiro, Phys. Rev. A **78**, 061802 (2008).
2. Y. Bromberg, O. Katz, and Y. Silberberg, Phys. Rev. A **79**, 053840 (2009).
3. Y. Zhang, J. Shi, H. Li, and G. Zeng, Chin. Opt. Lett. **12**, 073501 (2014).
4. L. Wang and S. Zhao, Photon. Res. **4**, 240 (2016).
5. I. M. Vellekoop and A. P. Mosk, Opt. Lett. **32**, 2309 (2007).
6. Z. Yin, G. Liu, F. Chen, and B. Liu, Chin. Opt. Lett. **13**, 071404 (2015).
7. R. Horstmeyer, H. W. Ruan, and C. H. Yang, Nat. Photon. **9**, 563 (2015).
8. L. Fang, C. Zhang, H. Zuo, J. Zhu, and L. Pang, Chin. Opt. Lett. **15**, 102901 (2017).
9. J. Bertolotti, E. G. van Putten, C. Blum, A. Lagendijk, W. L. Vos, and A. P. Mosk, Nature **491**, 232 (2012).
10. O. Katz, P. Heidmann, M. Fink, and S. Gigan, Nat. Photon. **8**, 784–790 (2014).
11. T. Wu, O. Katz, X. Shao, and S. Gigan, Opt. Lett. **41**, 5003 (2016).
12. C. W. J. Beenakker, Rev. Mod. Phys. **69**, 731 (1997).
13. S. M. Popoff, G. Lerosey, R. Carminati, M. Fink, A. C. Boccara, and S. Gigan, Phys. Rev. Lett. **104**, 100601 (2010).
14. S. Popoff, G. Lerosey, M. Fink, A. C. Boccara, and S. Gigan, Nat. Commun. **1**, 1 (2010).
15. Y. Choi, T. D. Yang, C. Fang-Yen, P. Kang, K. J. Lee, R. R. Dasari, M. S. Feld, and W. Choi, Phys. Rev. Lett. **107**, 023902 (2011).
16. J. Yoon, K. Lee, J. Park, and Y. Park, Opt. Express **23**, 10158 (2015).
17. M. Mounaix, D. Andreoli, H. Defienne, G. Volpe, O. Katz, S. Grésillon, and S. Gigan, Phys. Rev. Lett. **116**, 253901 (2016).
18. H. P. Paudel, C. Stockbridge, J. Mertz, and T. Bifano, Opt. Express **21**, 17299 (2013).
19. S. Tripathi, R. Paxman, T. Bifano, and K. C. Toussaint, Opt. Express **20**, 16067 (2012).
20. H. B. de Aguiar, S. Gigan, and S. Brasselet, Phys. Rev. A **94**, 043830 (2016).
21. T. Chaigne, O. Katz, A. C. Boccara, M. Fink, E. Bossy, and S. Gigan, Nat. Photon. **8**, 58 (2013).
22. Y. Park, W. Choi, Z. Yaqoob, R. R. Dasari, K. Badizadegan, and M. S. Feld, Opt. Express **17**, 12285 (2009).
23. Y. Choi, C. Yoon, M. Kim, T. D. Yang, C. Fang-Yen, R. R. Dasari, K. J. Lee, and W. Choi, Phys. Rev. Lett. **109**, 203901 (2012).
24. I. Yamaguchi and T. Zhang, Opt. Lett. **22**, 1268 (1997).
25. I. N. Papadopoulos, S. Farahi, C. Moser, and D. Psaltis, Biomed. Opt. Express **4**, 260 (2013).
26. M. Plöschner, T. Tyc, and T. Čižmá, Nat. Photon. **9**, 529 (2015).
27. D. Psaltis and C. Moser, Opt. Photon. News **27**, 24 (2016).